

Dynamic crossover in hydration water of curing cement paste: the effect of superplasticizer

This article has been downloaded from IOPscience. Please scroll down to see the full text article.

2012 J. Phys.: Condens. Matter 24 064108

(<http://iopscience.iop.org/0953-8984/24/6/064108>)

View [the table of contents for this issue](#), or go to the [journal homepage](#) for more

Download details:

IP Address: 129.6.122.169

The article was downloaded on 27/02/2012 at 18:10

Please note that [terms and conditions apply](#).

Dynamic crossover in hydration water of curing cement paste: the effect of superplasticizer

Hua Li^{1,2}, Wei-Shan Chiang¹, Emiliano Fratini³, Francesca Ridi³,
Francesco Bausi³, Piero Baglioni³, Madhu Tyagi^{4,5}
and Sow-Hsin Chen^{1,6}

¹ Department of Nuclear Science and Engineering, Massachusetts Institute of Technology, Cambridge, MA 02139, USA

² Department of Physics, Jinan University, Guangzhou 510632, People's Republic of China

³ Department of Chemistry and CSGI, University of Florence, via della Lastruccia 3-Sesto Fiorentino, I-50019 Florence, Italy

⁴ NIST Center for Neutron Research, Gaithersburg, MD 20899-1070, USA

⁵ Department of Materials Science and Engineering, University of Maryland, College Park, MD 20742, USA

E-mail: sowhsin@mit.edu

Received 6 May 2011, in final form 6 June 2011

Published 25 January 2012

Online at stacks.iop.org/JPhysCM/24/064108

Abstract

The influence of a new comb-shaped polycarboxylate-based superplasticizer (CSSP) on the hydration kinetics and transport properties of aged cement pastes has been investigated by high-resolution quasi-elastic neutron scattering (QENS) and low temperature differential scanning calorimetry (LT-DSC). A new method of analysis of QENS spectra is proposed. By applying the refined method we were able to access to four independent physical parameters including the self-diffusion coefficient of the hydration water confined in the cement paste. Mean squared displacement (MSD) of the hydrogen atom for mobile water molecules displays a dynamic crossover temperature in agreement with DSC data. The experimental results indicate that CSSP polymer added into cement paste moderates the hydration process and decreases the dynamic crossover temperature of the hydration water.

(Some figures in this article are in colour only in the electronic version)

1. Introduction

Superplasticizers (SPs) have been used for a long time in concrete technology to improve the workability of final cementitious admixtures. The main outcomes of the addition of these products to a cement paste are: the production of concretes with an extended time during which the material remains workable (i.e. self-compacting concrete) and the possibility to use very low water/cement ratios.

It is commonly accepted that SPs are adsorbed on the cement particles and act as dispersants by the resultant electrostatic and/or steric repulsion [1–3]. The workability (mainly apparent yield stress, lower viscosity for longer time,

concrete slump) of cement pastes and concretes containing SPs depends on the chemical composition of the admixture and on the molecular structure of the additive. However, the overall behavior of SPs is highly affected by the composition and size distribution of the cement used as well as by the hydrated phases formed during the early stage of hydration.

Nowadays, the latest generation of SPs is based on a class of comb-shaped polycarboxylate-based polymers. They have enhanced chemical characteristics that have been specifically tailored for the cement industry. In particular, they allow the resultant concretes to achieve very high compressive strength and extraordinary long-term durability.

In this regard, a detailed study has been conducted by Winnefeld *et al* [2] using a rather complete library of

⁶ Author to whom any correspondence should be addressed.

Table 1. The list of the hydrated cement pastes used in our QENS experiment.

Sample name	Age (setting time) of the hydrated cement
Sample A1	30 days hydrated cement with additive CSSP
Sample A2	14 days hydrated cement with additive CSSP
Sample A3	7 days hydrated cement with additive CSSP
Sample B1	30 days hydrated cement with no additive
Sample B2	14 days hydrated cement with no additive
Sample B3	7 days hydrated cement with no additive

comb-shaped polycarboxylate-ethers (i.e. different lengths and densities of side chains and total polymer molecular weight were considered) in order to demonstrate how the structure of the polymer controls both the rheology and the setting of the cement paste. As a result, polymers with higher molecular weight, lower side chain densities and shorter side chains adsorb more strongly to the dry grains, greatly influencing the rheological properties and setting times of the final cement paste. On the other hand, Flatt *et al* [3] examined the steric hindrance characteristics of similar comb-shaped polymers by using atomic force microscopy (AFM) directly on calcium silicate hydrate. As a main result, they were able to correlate the solution and surface properties of the comb copolymers with the force–distance curves obtained during AFM measurements through a scaling law approach. The proposed model represents the first successful attempt to quantitatively link the steric hindrance characteristic to the molecular structure (i.e. grafting density, and side chain and backbone length) of these dispersants.

The present investigation has been conducted on a comb-shaped polycarboxylate-based SP having a molecular macrostructure optimized to: achieve good workability, avoid undesirable retardation, and to obtain a high performance concrete.

In this paper, we investigated the single-particle dynamics and transport properties of hydration water as a function of aging (setting) time of cement pastes with and without CSSP additive at a constant temperature. Furthermore, we were able to identify the existence of a dynamic crossover temperature in the hydration water of all the aged cement pastes studied. Table 1 gives a list of all the aged cement pastes used in the present work. Details on the used cement and paste compositions can be found in section 2.

2. Experimental section

Cement with a specific surface area of $4604 \text{ cm}^2 \text{ g}^{-1}$ (Blaine) was obtained as a gift from CTG-Italcementi. Its composition in oxides is: SiO_2 16.7%, Al_2O_3 3.95%, Fe_2O_3 2.18%, CaO 66.3%, MgO 2.58%, SO_3 4.59%, Na_2O 0.58%, K_2O 0.86%, SrO 0.12% and Mn_2O_3 0.06%. Cement pastes were prepared by adding the exact amount of distilled water (or CSSP water solution) in order to have a w/c (water/dry cement ratio) of 0.31. CSSP was added in series A at 0.6% with respect to the mass of dry cement.

In the QENS experiment we used the high-flux backscattering spectrometer (HFBS) at NIST Center for

Neutron Research (NCNR) to determine the age dependence of the single-particle dynamics of water in the hydrated cement pastes with and without the additive. The spectrometer was used in two different modes: (i) with the Doppler stopped to measure the elastic scan as a function of temperature (25–290 K) and (ii) with the Doppler on at 24 Hz to extract the single-particle intermediate scattering function $F_T(Q, t)$ at a fixed temperature of 250 K. In this latter experimental set-up, the spectrometer has an energy resolution of $0.9 \mu\text{eV}$ and a dynamic range of $\pm 17 \mu\text{eV}$ which allows the measurement of the $F_T(Q, t)$ in the time range from 100 ps to 4 ns. The spectrometer has 16 detectors corresponding to 16 magnitudes of wavevector transfer Q values from 0.25 to 1.75 \AA^{-1} . An aluminum cylindrical sample cell of diameter 29 mm was used. All the investigated pastes (about 3 g) have been cured for different times from 7 to 30 days at 298 K in sealed plastic bags. Powders obtained by crushing the cured pastes were wrapped in a thin aluminum foil, which was then shaped in an annular fashion having the same inner circumference of the cylindrical sample holder. All the cells were loaded and sealed under helium gas to avoid any temperature gradient across the sample and also any loss of hydration water during the experiment. The transmission of the samples was about 90% which resulted in negligible multiple scattering contribution to the measured spectra.

DSC measurements were performed using a DSC Q -2000 from TA Instruments, and the data were elaborated with Q -Series software, version 5.2.4. Each measurement was carried out with the following temperature program: equilibrate to 278 K; cooling ramp from 278 to 193 K at 0.5 K min^{-1} . Cement pastes have been cast in sealed stainless-steel pans instead of standard Al pans to avoid any loss of water during the curing time. A thermostatic plate has been used to maintain the curing temperature exactly at 298 K when the pans were outside of the DSC instrument.

2.1. Model for QENS data analysis

In previous publications [4], we showed that hydration water dynamics in cement pastes can be described by a simple model where at a given time there are two categories of water molecules: a fraction p of immobile water molecules (immobile in the sense that the scattering from it appears as ‘elastic’ measured with a QENS spectrometer having an energy resolution in the μeV range) bound inside the hydration products, and a fraction $1 - p$ of mobile ‘glassy’ water molecules embedded in the amorphous gel region surrounding the hydration products. According to this picture, the translational part of the intermediate scattering function (ISF) of the water molecules in a cement paste can be written as follows:

$$F_T(Q, t) = p + (1 - p)F_v(Q, t) \exp[-(t/\tau_T(Q))^\beta] \quad (1)$$

where the factor $F_v(Q, t) \exp[-(t/\tau_T(Q))^\beta]$ represents the relaxation function of the mobile water according to the relaxing cage model (RCM) which was shown to well describe the single-particle dynamics of supercooled water [5] and of hydration water in Vycor glass [6]. β is

a phenomenological shape parameter associated with the deviation from a single exponential decay ($\beta = 1$), which is found in the event of a Debye-like process. In the present case the Kohlrausch–Williams–Watts (or stretched exponential) function is associated with a broad superposition of single exponential processes (in the ‘heterogeneous’ scenario framework) [7]. In fact, mobile water molecules sample the developing porosity and surface of the hydrated products which are heterogeneous in nature and evolve as time passes. The term ‘glassy’ is used to stress the experimental evidence that the relaxation process associated with the mobile water fraction is non-Debye-like (i.e. the relaxation function in the frequency domain is not a pure Lorentzian as expected for a Debye-like process) [8]. This model is valid for the description of low Q ($Q < 1 \text{ \AA}^{-1}$) scattering spectra from the ‘glassy’ water [5, 6]. It was shown that, for in this case, $F_v(Q, t)$ tends to a Debye–Waller factor asymptotically for large t , namely

$$F_v(Q, t) \underset{t > 1 \text{ ps}}{=} \exp(-Q^2 a^2 / 3), \quad (2)$$

where the vibrational amplitude a of a typical water molecule trapped in the tetrahedral hydrogen-bond cage is, to a good approximation, equal to 0.5 \AA for supercooled temperatures. Therefore for $Q < 1 \text{ \AA}^{-1}$ the $F_v(Q, t)$ is numerically essentially equal to unity in practice. The essence of the RCM states that the Q -dependent translational relaxation time is given by $\tau_T(Q) = \tau_0(aQ)^{-\gamma}$. In RCM, both the exponents β and γ are Q -dependent [6]. But in the hydrodynamic limit ($Q \rightarrow 0$ limit), $\beta \rightarrow 1$, $\gamma \rightarrow 2$, and we demand that

$$\exp[-(t/\tau_T(Q))^\beta] = \exp[-(t/\tau_0)^\beta (aQ)^{\beta\gamma}] \xrightarrow{Q \rightarrow 0} \exp[-DQ^2 t]. \quad (3)$$

From this consideration we identify the average translational relaxation time $\langle \tau \rangle$ and the self-diffusion coefficient D of the water molecule, respectively, as

$$\langle \tau \rangle = \int_0^\infty dt \exp[-(t/\tau_T(Q))^\beta] = \frac{1}{\beta} \Gamma\left(\frac{1}{\beta}\right) \tau_0, \quad D = \frac{a^2}{\tau_0}. \quad (4)$$

It should be noted here that the latter expression for D is a new relation derived in our new and improved RCM. Thus, aside from p , we are able to derive three physical parameters β , $\langle \tau \rangle$ and D for the mobile fraction of hydration water from the two original independent parameters β and τ_0 in the RCM. Furthermore, if we regard $\langle \tau \rangle$ as a quantity which is proportional to the structural relaxation time and thus also proportional to the shear viscosity, then in the temperature range where the Stokes–Einstein relation is valid, we should have a relation $D\langle \tau \rangle / T = \text{constant}$ [9]. We shall see later (table 2) that this relation is, in fact, satisfied to within 10% from our QENS data taken at $T = 250 \text{ K}$.

3. Result and discussion

A measured QENS spectrum at magnitude of wavevector transfer Q and energy transfer E is first corrected for background and for detector efficiency and then its area normalized to unity. The resulting spectrum is then

Table 2. The values of parameters for the six cement samples investigated.

Hydrated cement + SP	Sample A1	Sample A2	Sample A3
β	0.71	0.75	0.69
$D\langle \tau \rangle (\text{\AA}^2)$	0.37	0.33	0.36
Hydrated cement	Sample B1	Sample B2	Sample B3
β	0.65	0.61	0.67
$D\langle \tau \rangle (\text{\AA}^2)$	0.46	0.41	0.36

numerically Fourier-transformed to a time domain function $F_M(Q, t)$. This function is then corrected for the measured energy resolution at this Q by dividing it by the corresponding time domain resolution function to obtain the total single-particle intermediate scattering function $F_T(Q, t)$. This is a time domain function that we can fit with the model given by equation (1).

The red circle points in figures 1(a) and (b) show the so-obtained $F_T(Q, t)$ as a function of t at two distinct Q values, 0.56 and 0.99 \AA^{-1} . The blue solid lines show the results of the model fitting using equation (1). The red circular points in the second and third panels in figures 1(a) and (b) are the corrected and normalized neutron spectra. The solid green lines are the model fitting results in the energy domain. The normalized spectra can be decomposed into a sum of an elastic neutron scattering (ENS) line (the blue solid lines) and a quasi-elastic line (the black solid lines). In general, the Q -dependent correlation time $\tau_T(Q) = \tau_0(aQ)^{-\gamma}$, so as Q increases the correlation time becomes shorter (as shown in the right panel of figure 2) and therefore the corresponding spectrum becomes broader.

The left panels of figure 2 display the three physical parameters: the elastic fraction p , the averaged translational relaxation time $\langle \tau \rangle$ and the self-diffusion coefficient D for a water molecule within the mobile fraction, as calculated from the extracted RCM parameters. The right panel of figure 2 depicts the power-law Q dependence of the Q -dependent translational relaxation time $\tau_T(Q)$.

Figure 3 displays the mean squared displacement (MSD) of a hydrogen atom of the typical mobile water molecule in the cement pastes extracted from an elastic scan of the backscattering spectrometer, HFBS. It is clearly seen that the temperature dependence of the MSD shows a well-defined crossover phenomenon (exhibited as an abrupt change of slope), which agrees qualitatively with the peak position (T_L) of the LT-DSC cooling scans (see figure 5). Figure 3 shows that the crossover temperature slightly increases with the aging time. Also, with additives, the crossover temperature becomes slightly lower.

Figure 4 shows the evolution of the free water index (FWI) for the two samples compared to the $(1 - p)$ versus time behavior. The FWI parameter has been calculated by integration of the melting peak of the water in the heating scan of the LT-DSC measurements, as described in the literature [10, 11]. The FWI parameter decreases as time passes because available water molecules are gradually converted into the hydrated products by the hydration reaction. The

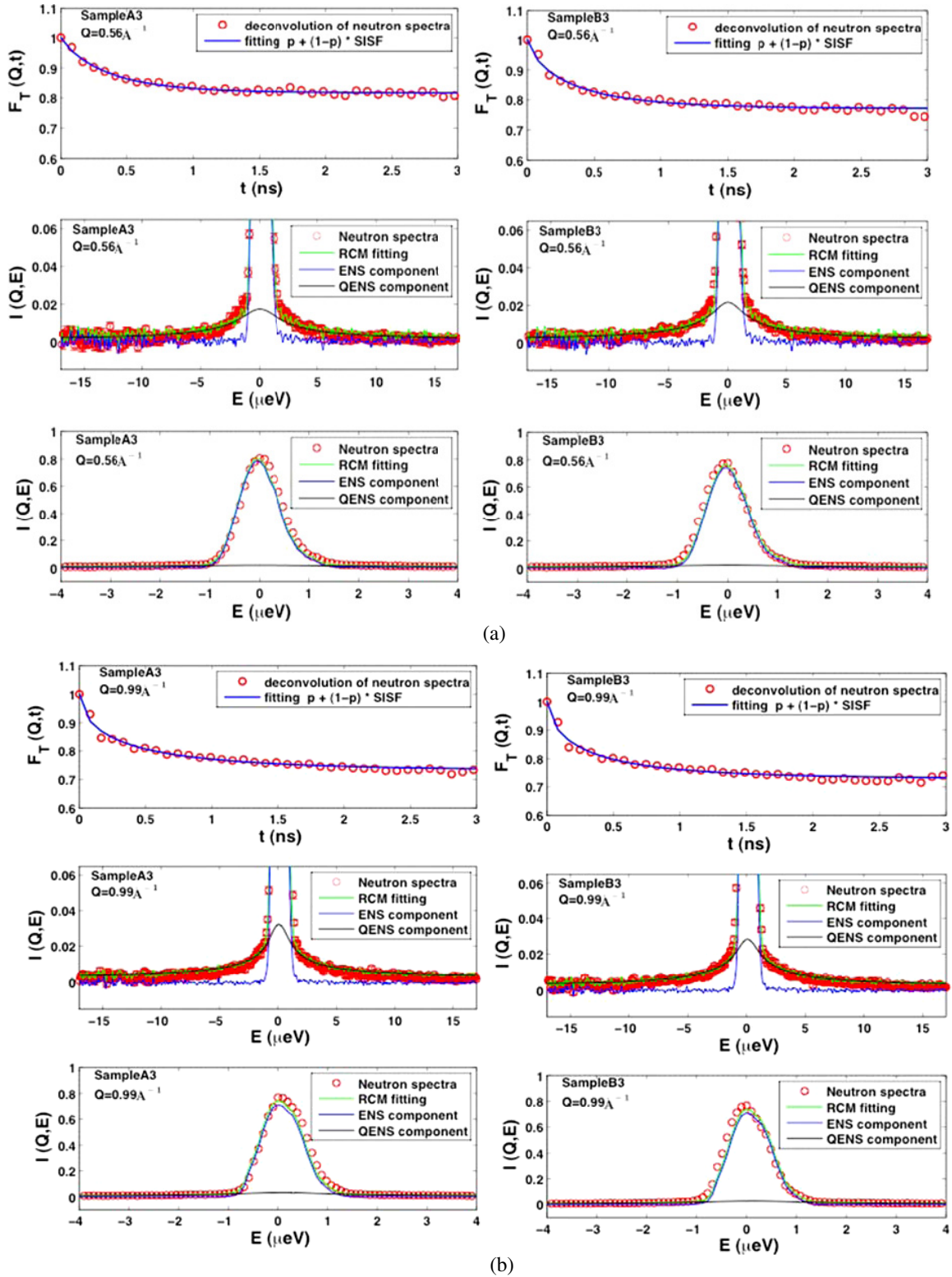


Figure 1. (a) Examples of the model fitting of QENS spectra taken at $Q = 0.56 \text{ \AA}^{-1}$. Left-hand side panel refers to data from sample A3 (a sample having an age of 7 days with the additive). Right-hand side panel refers to data from sample B3 (a sample having an age of 7 days without the additive). In each panel the top figure is the intermediate scattering function obtained from Fourier transform of the measured self-dynamic structure factor after deconvolution of the measured resolution function. The second and third panels on the left and on the right sides show the level of agreement between the measured spectrum and the model. The error bars throughout the text represent one standard deviation and are smaller than the circle. (b) Another example of the model fitting of QENS spectra taken at $Q = 0.99 \text{ \AA}^{-1}$. Left-hand side panel refers to data from sample A3 (a sample having an age of 7 days with the additive). Right-hand side panel refers to data from sample B3 (a sample having an age of 7 days without the additive). In each panel the top figure is the intermediate scattering function obtained from Fourier transform of the measured self-dynamic structure factor after deconvolution of the measured resolution function. The second and third panels on the left and on the right sides show the level of agreement between the measured spectrum and the model. The error bars throughout the text represent one standard deviation and are smaller than the circle.

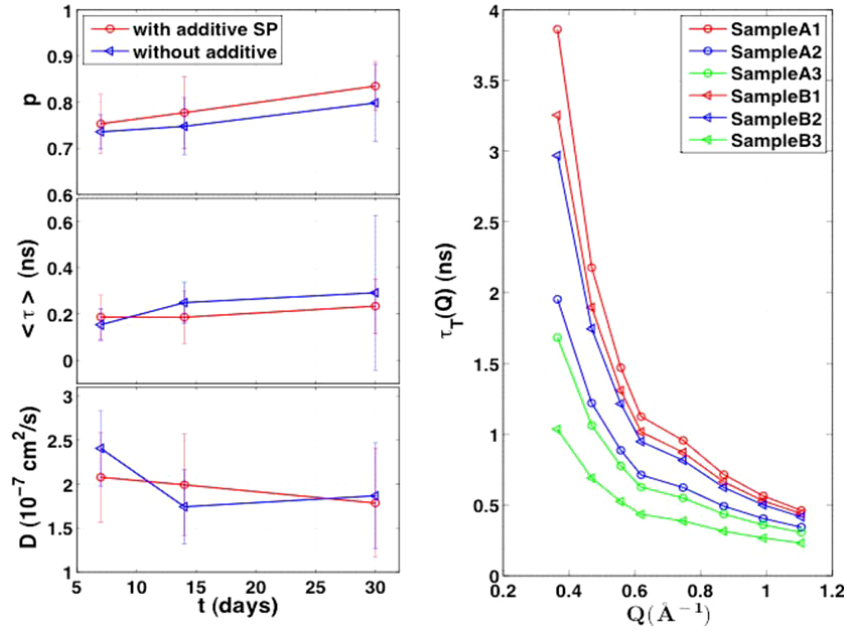


Figure 2. The left panels show the three physical parameters obtained from fitting the spectra by the model as a function of age of the cement paste used in our experiment: the elastic fraction, p ; the averaged translational relaxation time, $\langle \tau \rangle = (\frac{\tau_0}{\beta})\Gamma(\frac{1}{\beta})$; the self-diffusion constant, $D = \frac{2.5}{\tau_0(\text{ns})} \times 10^{-8} \text{ cm}^2 \text{ s}^{-1}$. The right panel gives the Q -dependent relaxation time $\tau_T(Q) = \tau_0(aQ)^{-\gamma}$. In the left panels, the red circles refer to samples with the additive SP and blue triangles to samples without the additive. The solid lines are for guides for the eyes. It is clear from the right panel that $\tau_T(Q)$ has a power-law dependence on Q .

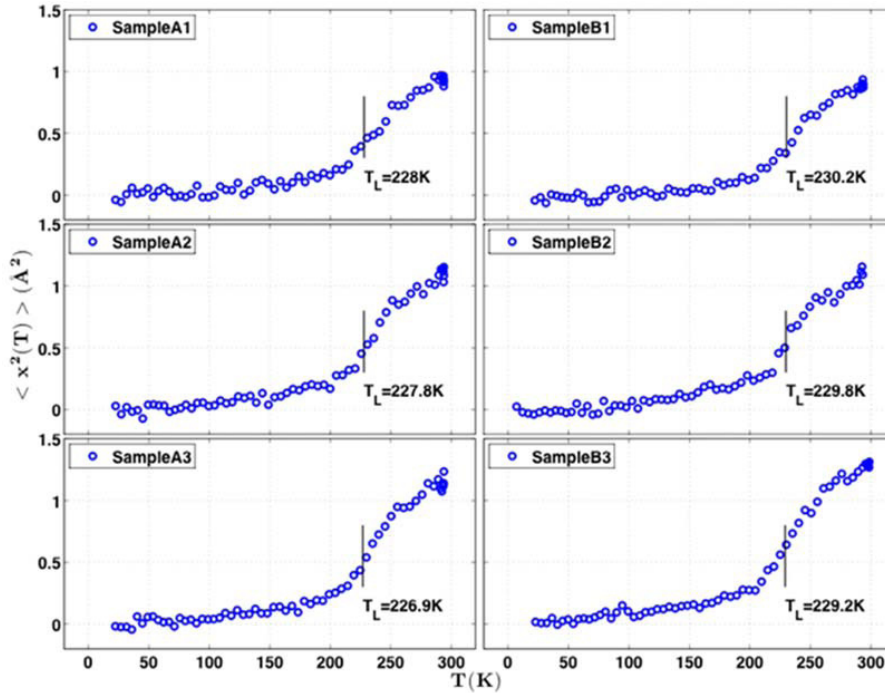


Figure 3. The mean squared displacement (MSD) of the hydrogen atom for mobile water molecules in curing cement pastes A1, A2, A3, B1, B2 and B3 as a function of temperature. Each MSD shows a characteristic dynamic crossover phenomenon at a crossover temperature, which approximately coincides with the peak position T_L in the LT-DSC cooling scan shown in figure 5.

FWI values of the cement and of the cement/CSSP pastes are very different after one day of hydration, because the superplasticizer retards the water consumption. However, after three days their FWI values almost coincide and keep on diminishing slightly up to 30 days. The decrease of FWI

is somewhat steeper in the cement/CSSP case. The same behavior is observed for the $(1 - p)$ values, as reported in the graph.

It is worth mentioning that the QENS technique in backscattering geometry does not allow following the bulk

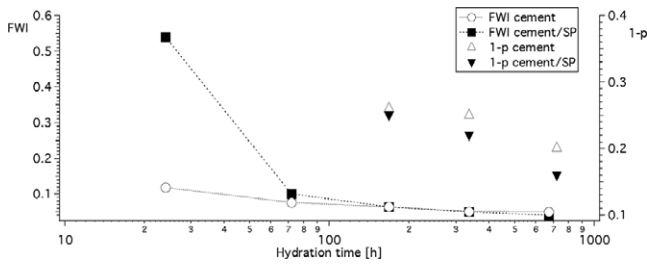


Figure 4. FWI and $(1 - p)$ versus hydration time (the age) for the cement paste (white symbols) and for the cement/CSSP paste (black symbols).

water dynamics at room temperature since the water relaxation times are shorter than 100 ps (i.e. the lowest relaxation time accessible by HFBS). On the other hand, when bulk water is converted into ice the relaxation times become longer than 4 ns (i.e. only an elastic peak is obtained). For this given reason the cement pastes with hydration times shorter than 3 days have not been studied by QENS but monitored by LT-DSC.

Figure 5 shows LT-DSC cooling scans recorded during the hydration of cement (left panel) and cement/CSSP (right panel) pastes. According to the colloidal model, [12] the porosity of a cement paste can be classified into three different categories addressable by means of LT-DSC. In the capillary pores, typically larger than 10 nm, water still behaves as bulk water and an example is shown by the very sharp peak at 257 K in the case of cement/CSSP just after 1 day of curing (see right panel of figure 5). In large gel pores (LGP), whose dimensions range between 3 and 10 nm, water freezes in the 238/248 K temperature interval [13]. Finally, water freezes below 238 K when it is confined within small gel pores (SGP), typically corresponding to 1–3 nm in diameter. Considering the hydration of plain cement (see the left panel of figure 5),

after one day, the thermogram displays a group of exothermic peaks with an onset at 246 K, due to water confined within both LGP and SGP. After 3 days of curing, the peak around 243 K is hardly detectable, completely disappearing after 7 days as evidence of the fact that the water confined within LGP is entirely consumed by the hydration reaction. In the thermograms from 7 up to 28 days, only the peak belonging to SGP-water is present, with a maximum at about 230 K. The addition of the CSSP to the cement paste modifies the setting process (see the right panel of figure 5). In fact, bulk water is still present even after 1 day as shown by the sharp peak around 257 K. No other peaks are detected at this stage, indicating that the cement microstructure has not yet formed. After 3 days, both the SGP and LGP peaks are evident, with the latter disappearing after 7 days. Again at a curing time longer than 7 days, only the SGP-water is present in the cement paste as testified by the peak at about 228 K. The CSSP retards the water consumption but it does not change the microstructural evolution of the developing hydrated phases.

The state of the water confined in the porosity of a curing cement paste was previously investigated as a function of hydration time by the combined use of LT-DSC and near-infrared spectroscopy (NIR) [13]. The NIR investigation was of utmost importance since both QENS and DSC cannot provide direct information on the structure of the unreacted water at low temperature. In particular, NIR showed that, when water is completely confined (SGP, 1–3 nm), its crystallization to hexagonal ice is prevented in favor of an amorphous water state which is in agreement with an FSC [14, 15].

Table 2 lists the shape parameter, β which is an indicator of the degree of the heterogeneity of pore sizes in which the CSH gel is confined. The broader the pore size distribution, the lower the values of β . From table 2 it is evident that the pore size distribution is narrower in the case of cement + SP

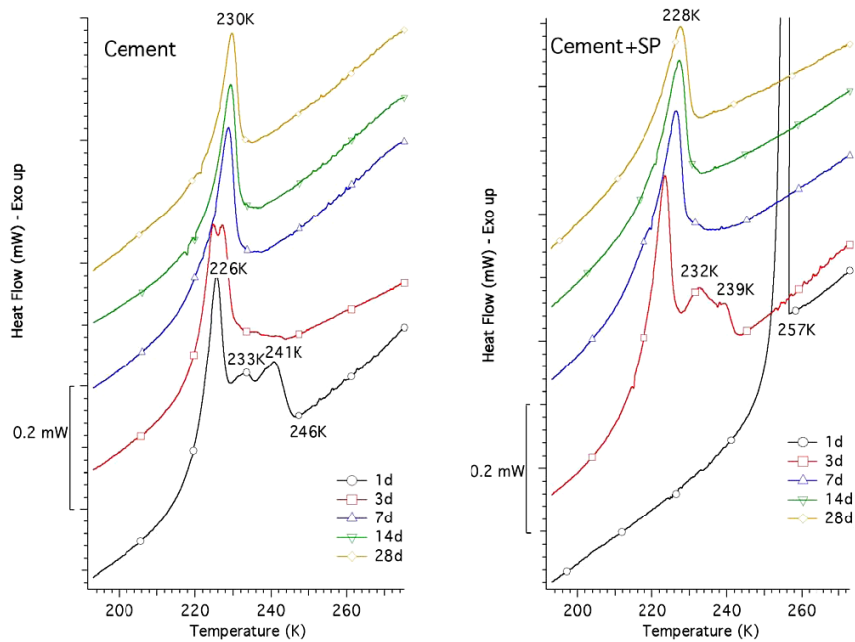


Figure 5. LT-DSC thermograms recorded on cement pastes at different curing times after mixing without additive (left panel) and with CSSP additive (right panel).

because the β value is higher with the A series of samples. In the same table the values of the product $D\langle\tau\rangle$ are also reported for each sample of the two series (A and B). In all cases at $T = 250$ K, the before-mentioned product is approximately constant to within 10%, indicating the validity of the Stokes–Einstein relation for the unreacted water confined in cement pastes.

4. Summary

We analyzed measured QENS spectra of cured cement pastes with an improved model using time domain methodology. We extract four physical parameters: p , β , $\langle\tau\rangle$ and D and show the existence of a crossover temperature from the T -dependent MSD data for the mobile fraction of the hydration water in all investigated cases. We demonstrate that $1 - p$ is related to the FWI as determined by LT-DSC and the crossover temperature is consistent with the position of the LT-DSC peak related to the water strongly confined in the small gel porosity proper of a cured cement paste. We further argue that the average translational relaxation time $\langle\tau\rangle$ is proportional to the structural relaxation time and hence also to the shear viscosity. This argument is valid based on the experimental fact that the Stokes–Einstein relation, $D\langle\tau\rangle/T = \text{const}$, is satisfied.

Acknowledgments

The research at MIT is supported by DOE grant no. DE-FG02-90ER45429. This work utilized facilities supported in part by the National Science Foundation under agreement no. DMR-094477. HL acknowledges the hospitality of the Department of Nuclear Science and Engineering of MIT during her stay as a Visiting Scientist. EF, FR, FB and PB gratefully acknowledge the Ministero dell’Istruzione, Università e della Ricerca Scientifica (MIUR, grant PRIN-2008, prot. 20087K9A2J), Consorzio Interuniversitario per lo Sviluppo dei Sistemi a Grande Interfase (CSGI) and CTG-Italcementi for partial financial support to this project. We thank NIST Center For Neutron Research for allocation of neutron beam time in HFBS. The cement (Blaine) is identified in this paper to foster understanding. Such identification does not imply recommendation or endorsement by NIST, nor does it imply that the material identified is necessarily the best available for the purpose.

References

- [1] Uchikawa H, Hanehara S and Sawaki D 1997 The role of steric repulsive force in the dispersion of cement particles in fresh

paste prepared with organic admixture *Cement Concr. Res.* **27** 37–50

- [2] Winnefeld F, Becker S, Pakusch J and Goetz T 2007 Effects of the molecular architecture of comb-shaped superplasticizers on their performance in cementitious systems *Cement Concr. Composites* **29** 251–62
- [3] Flatt R J, Schober I, Raphael E, Plassard C and Lesniewska E 2009 Conformation of adsorbed comb copolymer dispersants *Langmuir* **25** 845–55
- [4] Fratini E, Chen S-H, Baglioni P and Bellissent-Funel M-C 2001 Age-dependent dynamics of water in hydrated cement paste *Phys. Rev. E* **64** 020201(R)
- Ridi F, Fratini E and Baglioni P 2011 *J. Colloid Interface Sci.* **357** 255–64
- [5] Chen S-H, Liao C, Sciortino F, Gallo P and Tartaglia P 1999 Models for single-particle dynamics in supercooled water *Phys. Rev. E* **59** 6708–14
- [6] Zannoti J M, Bellissent-Funel M-C and Chen S-H 1999 Relaxational dynamics of supercooled water in porous glass *Phys. Rev. E* **59** 3084–93
- [7] Arbe A, Colmenero J, Monkenbusch M and Richter D 1998 Dynamics of glass-forming polymers: homogeneous versus ‘heterogeneous’ scenario *Phys. Rev. Lett.* **81** 590–3
- [8] Fratini E, Chen S-H, Baglioni P and Bellissent-Funel M-C 2002 Quasi-elastic neutron scattering study of diffusional dynamics of hydration water in tricalcium silicate *J. Phys. Chem. B* **106** 158–66
- [9] Chen S-H, Mallamace F, Mou C-Y, Broccio M, Corsaro C, Faraone A and Liu L 2006 The violation of Stokes–Einstein relation in supercooled water *Proc. Natl Acad. Sci. USA* **103** 12974–8
- [10] Damasceni A, Dei L, Fratini E, Ridi F, Chen S-H and Baglioni P 2002 A novel approach based on differential scanning calorimetry applied to the study of tricalcium silicate hydration kinetics *J. Phys. Chem. B* **106** 11572–8
- [11] Ridi F, Dei L, Fratini E, Chen S-H and Baglioni P 2003 Hydration kinetics of tri-calcium silicate in the presence of superplasticizers *J. Phys. Chem. B* **107** 1056–61
- [12] Jennings H M 2000 A model for the microstructure of calcium silicate hydrate in cement paste *Cement Concr. Res.* **30** 101–16
- Jennings H M 2008 *Cement Concr. Res.* **38** 275–89
- [13] Ridi F, Luciani P, Fratini E and Baglioni P 2009 Water confined in cement pastes as a probe of cement microstructure evolution *J. Phys. Chem. B* **113** 3080–7
- [14] Zhang Y, Lagi M, Ridi F, Fratini E, Baglioni P, Mamontov E and Chen S-H 2008 Observation of dynamic crossover and dynamic heterogeneity in hydration water confined in aged cement paste *J. Phys.: Condens. Matter* **20** 502101
- [15] Zhang Y, Lagi M, Fratini E, Baglioni P, Mamontov E and Chen S-H 2009 Dynamic susceptibility of supercooled water and its relation to the dynamic crossover phenomenon *Phys. Rev. E* **79** 040201(R)